HEAT INPUT EFFECT OF FRICTION STIR WELDING ON ALUMINIUM ALLOY AA 6061-T6 WELDED JOINT

Andrijana Djurdjevic[1], Srdjan Tadic[1], Ratnesh Kumar[2], Somnath Chattopadhyaya[12] Sergej Hloch[3,4], Aleksandar Sedmak[5], Elisaveta Donceva[6]

[1]Innovation Center of the Faculty of Mechanical Engineering, Kraljice Marije 16, Belgrade, Serbia
[2]Department of Mechanical Engineering, ISM Dhanbad, India
[3]Faculty of Manufacturing Technologies, Technical university of Kosice with a seat in Presov, Slovakia
[4]Institute of Geonics AS CR, v.v.i., Ostrava, The Czech Republic
[5]University of Belgrade, Faculty of Mechanical Engineering, Kraljice Marije 16, Belgrade, Serbia
[6]University of Skopje, Faculty of Mechanical Engineering, Skopje, Macedonia
E-mail: asedmak@mas.bg.ac.rs

Abstract: -This paper deals with the heat input and maximum temperature developed during friction stir welding with different parameters. Aluminium alloy (AA 6061-T6) has been used for experimental and numerical analysis. Experimental analysis is based on temperature measurements by using infrared camera, whereas numerical analysis was based on empirical expressions and finite element method. Different types of defects have been observed in respect to different levels of heat input.

Key-words: - Friction stir welding (FSW), Defect, Heat input, Maximum Temperature

1. Introduction

Friction stir welding quality is determined and controlled by the heat generated during process, which is determined by parameters like rotational speed, welding speed, plunge depth etc. Figure 1 shows the schematically the friction stir welding process, including non-consumable rotational tool which plunges through the material, generating heat due to contact between tool and work piece and bringing material into a semi solid state. Due to stirring action and consolidated pressure by the tool material gets joined, [1].

Podrzaj P. et al studied different types of defects at friction stir welding, like tunnels, voids, surface grooves, excessive flash, surface galling, nugget collapse and kissing bond. They indicated the heat input as main reason for these defects, [2]. There are many different ways to evaluate heat input during FSW, including analytical ones, as shown in [3], used also for numerical evaluation of temperature distribution, as shown in [4-5]. Regarding experimental investigations, the maximum temperature has been recorded, as the measure of heat input, which makes sense also from material science point of view, because eventual defects are direct consequence of temperature changes. Both numerical, the finite element method (FEM), and experimental investigations, using thermocouples, are presented in [6-9].

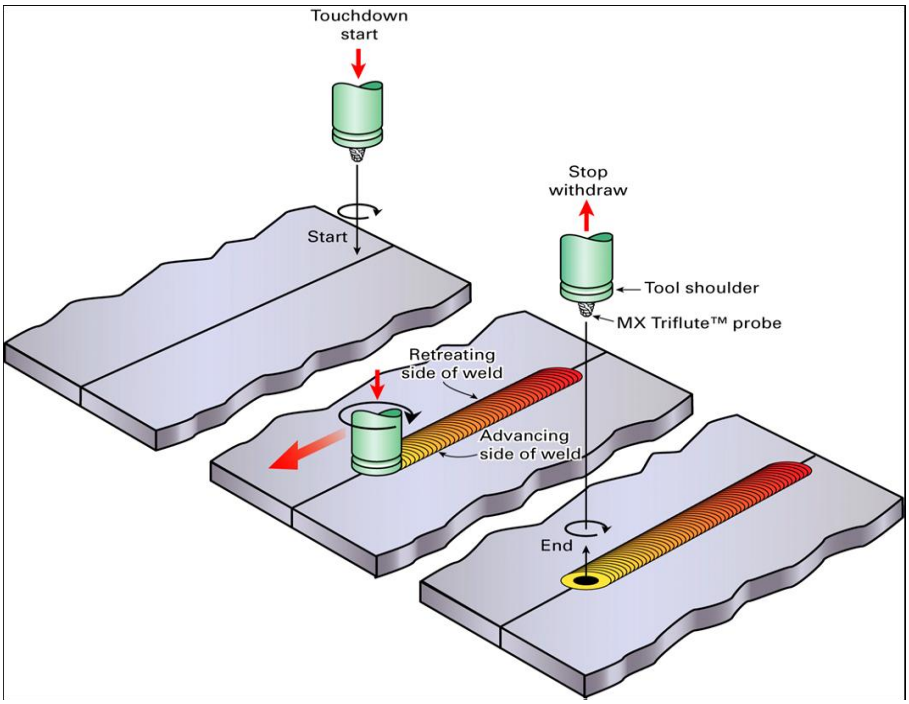

Figure 1. Schematic drawing of friction stir welding, [10].

The aim of this study is to investigate the different weld defects generated in aluminium alloy 6061 T6 due to different heat inputs. Toward this aim both numerical and experimental procedures are applied to evaluate maximum temperature and heat input for different welding parameters.

2. Experimental and numerical results

Table 1 shows FSW parameters for 4 different welded samples and corresponding maximum temperatures, as measured by infrared camera (CHAUVIN ARNOX C.A. 1888). Typical output (thermal image) from the infrared camera is shown in Fig. 2, indicating maximum temperature 514.74 ^{0}C (sample 4, Table 1).

Table 1. Friction stir welding parameters and resulting maximum temperatures

Sample No.	Rotational Speed (rpm)	Welding Speed (mm/min)	Maximum Temperature, ^{0}C
1	500	25	482 (measured)
2	710	25	519 (measured)
3	1000	25	539 (measured)
4	710	40	515 (measured)
5	500	40	479 (calculated)

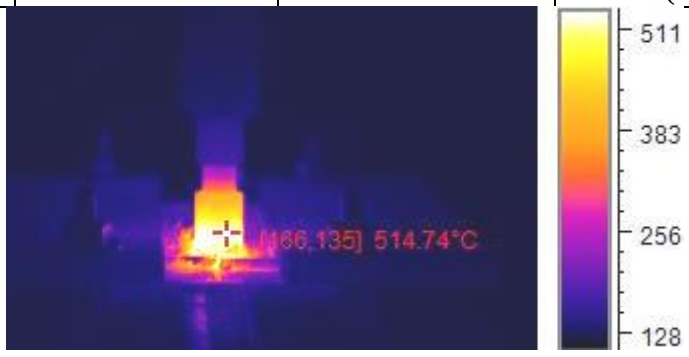

Figure 2. Infrared thermal image of FSW process.

One of the simplest ways to calculate the maximum temperature is to use equation based on the ratio of rotational (ω) and welding (ν) speed, as given in [11]:

$$\frac{T}{T_{melt}} = K\left(\frac{\omega^2}{\nu \cdot 10^4}\right)^{\alpha} \tag{1}$$

where T and T_{melt} are the maximum and melting temperature (^oC), respectively, 0,65<K< 0,75 and 0,04<α<0,06 the fitting constants. Higher FSW temperatures are obviously linked to the increasing rotational speed and decreasing welding speed. Also, it might be noticed that welding temperature is much more influenced by rotational speed than the welding speed. Experimental temperatures measurements, presented in Table 1, are examined in terms of Equation 1. The result of such examination is shown in Fig. 3, where the least squares analysis has been performed over the experimental data. Linear correlation has been revealed to be in a good agreement with the results, the scatter being less than ± 20 ^oC at low 'heat input'point, sp.1-1. The least square analysis suggests that the measured maximum temperatures were in the upper bound (K=0,745≈0,75), or even above it (α=0,069≈0,07), of the values proposed by Equation 1. Therefore, by using eq. (1), one gets the approximate correlation between the maximum temperature and basic welding parameters, i.e. heat input:

$$\frac{T}{T_{melt}} = 0.75\left(\frac{\omega^2}{\nu \cdot 10^4}\right)^{0.07} \tag{1a}$$

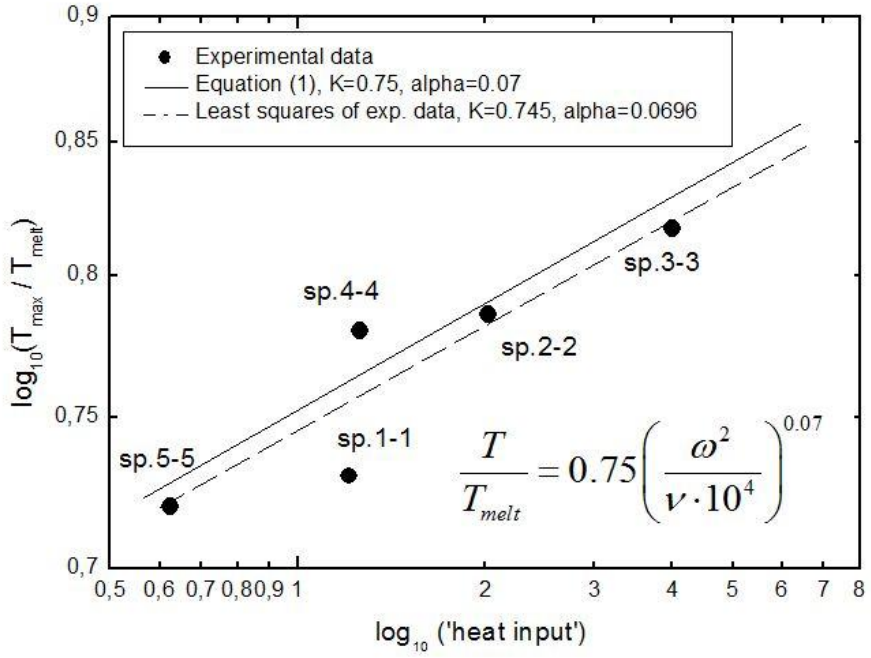

Figure 3. The least squares analysis of measured peak temperature, Table 1.

Equation 1 emphasises the influence of the two main processing variables - rotational and welding speed - on the maximum FSW temperature. However, more accurate assessment reveals that total heat input is much more complex phenomenon, depending on a number of variables. In this paper, two-dimensional finite elements analysis has been performed in order to clarify temperature distribution

during the FSW of the investigated aluminium AA 6061-T6 alloy. The self-made software has been used, based on open source FEM solver Code Aster. The total heat flux has been split into the shoulder-flux (friction driven) and pin-flux (plasticity driven), [3]:

$$q = q_{sh} + q_{pin} = 2\pi\mu F_n r_{sh}\omega + \frac{2\pi\bar{\sigma}h_p r_p \omega}{\sqrt{3\left(1+\mu^2\right)}} \tag{2}$$

Geometrical set-up, mesh, boundary values and initial condition are shown in Fig. 4. Free surfaces were supposed to obey convection boundary conditions – upper surface exposed to room temperature air; the bottom surface in a firm contact with stainless steel L-316 back plate. All material and thermodynamic parameters were used as a literature data typical for 6061 Al-alloy, [3]. Computational results are shown in Fig. 5, indicating that the maximum temperatures (647 ^{0}C) appear under the shoulder and near the pin, which were not reachable by infrared camera. However, the measurable area, behind the shoulder is, on average value, in good agreement with infrared camera results, indicating 550 ^{0}C.

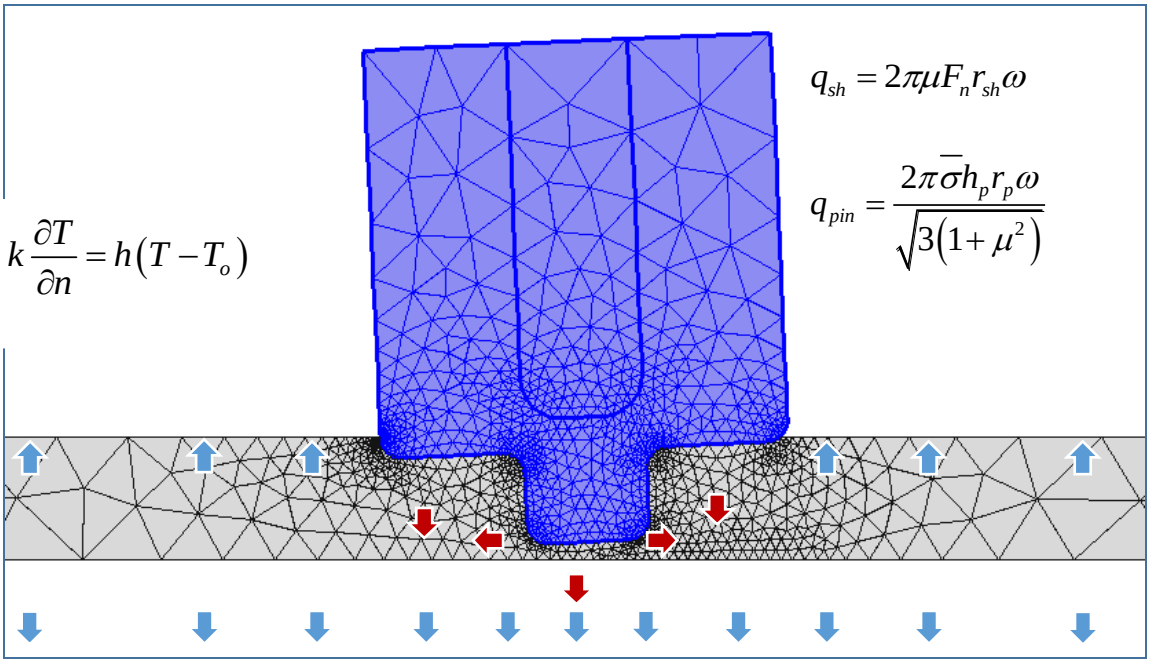

Figure 4. Geometry and mesh setup of the FEM analysis.
Boundary conditions (heat input and output are illustrated by red and blue arrows.

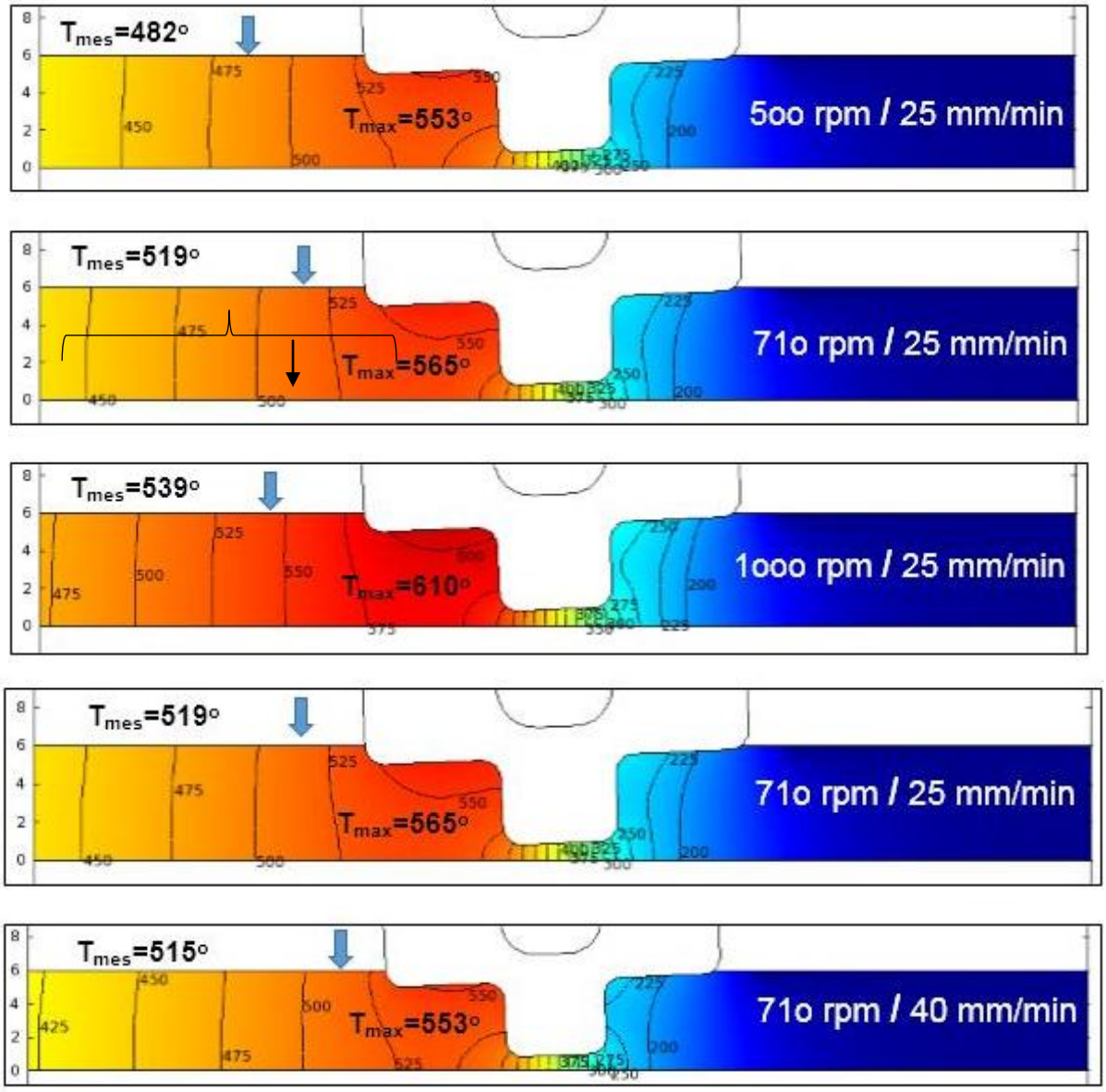

Figure 5. Temperature distribution (FEM study) for different welding parameters.

3. Defects in welded sample vs. heat input

After welding the samples through visual inspection defects are observed on the welded plates. Typical defects caused by excessive and insufficient heat are shown and analysed here, Figs. 6 and 7, respectively. When tool is taken out of the workpiece as an exit hole is left, as shown in Fig. 6 for sample 3.

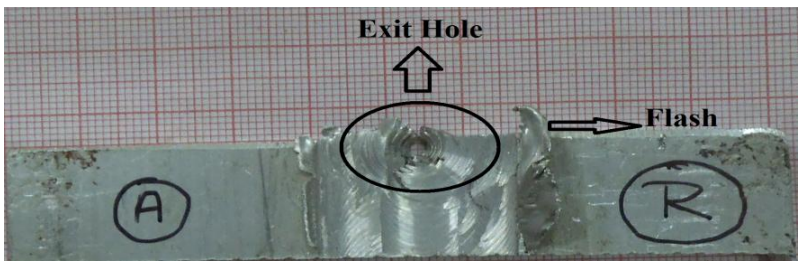

Figure 6. Exit hole and flash.

Exit hole phenomena is observed during all the process parameters, so that certain amount of material is wasted every time. It is observed that size of exit hole is equal to that of pin size. In Fig. 6, shown for the sample 3 (Table 1), extra material is observed in the weld joint area, known as flash. The reason for the flash formation is the excessive heat generation causing excessive thermal softening of the workpiece beyond the boundary of tool shoulder, also shown in [2]. Hence upper layer of the material come out forming an excessive surface known as flash. Consequently this leads to the thinning of the material in the weld area. Hence at the weld root area, pin starts making contact with the backing bar which causes rupture of material.

Contrary to that, material doesn't become soft enough in the case of insufficient heat input. Hence the tool is not able to stir and mix the material, resulting in improper weld. In Fig. 7, which shows the welded joint made with tool rotational speed 500 rpm and weld speed 40 mm/min (sample 5), irregular weld surface can be observed from the visual inspection. The reason for such surface is less heat generation due to lower rotational speed and high welding speed, as shown also in [2].

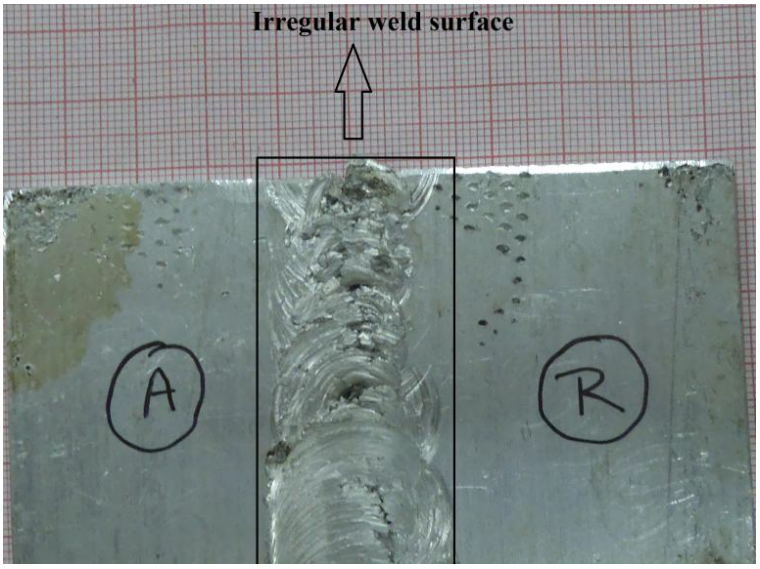

Figure 7. Irregular weld surface due to insufficient heat input.

4. Conclusions

From the above study of the heat input and weld defects due to friction stir welding of AA 6061-T6 one can conclude the following:

- Measured and calculated values of the maximum temperature are in good agreement, if one takes into account the location of infrared camera measurement.
- Equation (1) is useful analytical tool for simple evaluation maximum temperature depending on basic FSW parameters (rotational and welding speed)
- Weld defects, observed in this study, are typical for excessive and insufficient heat inputs.
- One can use this study to predict FSW parameters needed for sound welded joint.

5. References

1. B.T. Gibson et al, Friction stir welding: process, automation and control, Journal of Manufacturing Processes 16 (2004), pp. 56-73
2. P. Podrzaj, B. Jerman, D. Klobcar, Welding defects at friction stir welding, Metalurgija 54 (2015), 2, pp. 387-389
3. H. Schmidt, J. Hattel, J. Wert, An analytical model for the heat generation in friction stir welding. Model Simul Mater Sci Eng 12 (2004), pp. 143–157
4. Darko M. Veljić, Milenko M. Perović, Aleksandar S. Sedmak, Marko P. Rakin, Miroslav V. Trifunović, Nikola S. Bajić and Darko M. Bajić, A Coupled Thermo-mechanical Model of Friction Stir Welding, THERMAL SCIENCE 16 (2012), 2, pp. 527-534
5. D. Veljic, A. Sedmak, M. Rakin, N. Bajic, B. Medjo, D. Bajic, V. Grabulov, Experimental and Numerical Thermo-Mechanical Analysis of Friction Stir Welding of High Strength Aluminium Alloy, THERMAL SCIENCE 18 (2014), Suppl. 1, pp. S29-S38
6. M. Song, R. Kovačević, Numerical and Experimental Study of the Heat Transfer Process in Friction Stir Welding, Journal of Engineering Manufacture, 217 (2003), 1, pp. 73-85
7. C.M. Chen, R. Kovacevic Finite element modeling of friction stir welding - thermal and thermo-mechanical analysis. Int J Mach Tools Manuf. 43 (2003), pp. 1319–1326
8. A.M.M. Eramah, S. Tadić, A. Sedmak, Impact Fracture Response of Friction Stir Welded Al-Mg Alloy, Structural Integrity and Life, Vol. 13 (2013), 3, p. 171-177
9. D. Veljić, M. Perović, A. Sedmak, M. Rakin, N. Bajić, B. Medjo, H. Dascau, Numerical Simulation of the Plunge Stage in Friction Stir Welding, Structural Integrity and Life, Vol.11, (2011), 2, pp.131-134
10. http://www.esab.de/de/de/support/upload/FSW-Technical-Handbook.pdf
11. H. Bisadi, A. Tavakoli, M. T. Sangsaraki, K. T. Saragaraki; Materials and Design, (2013), pp. 80–88.